SHOCK-INITIATED IGNITION FOR HYDROGEN MIXTURES OF DIFFERENT CONCENTRATIONS

Melguizo-Gavilanes, J. and Bauwens, L.

Department of Mechanical and Manufacturing Engineering,
University of Calgary, Calgary AB T2N 1N4, Canada, jmelguiz@ucalgary.ca

ABSTRACT

The scenario of ignition of fuels by the passage of shock waves is relevant from the perspective of safety, primarily because shock ignition potentially plays an important role in deflagration to detonation transition. Even in one dimension, simulation of ignition between a contact surface or a flame and a shock moving into combustible mixture is difficult because of the singular nature of the initial conditions. Indeed, initially, as the shock starts moving away from the contact surface, the region filled with shocked reactive mixture does not exist. In the current work, the formulation is transformed, using time and length over time as the independent variables. This transformation yields a finite domain from $t = 0$. In this paper, the complete spatial and temporal ignition evolution of hydrogen combustible mixtures of different concentrations is studied numerically. Integration of the governing equations is performed using an Essentially Non-Oscillatory (ENO) algorithm in space and Runge-Kutta in time, while the chemistry is modeled by a three-step chain-branching mechanism which appropriately mimics hydrogen combustion.

1. INTRODUCTION

The risk of detonation for hydrogen mixtures remains an issue from the standpoint of hydrogen safety, especially in enclosed environments such as tunnels and garages. Heating of reactive mixture by the passage of shock waves and shock reflections may play an important role in the deflagration to detonation transition (DDT) process.

The initial value problem solved represents either a shock that reflected from a wall, or a shock that came from inert/burnt mixture at high temperature, and propagates into fresh reactive mixture at a lower temperature. Physically, the latter case represents a shock crossing over a flame, neglecting the flame propagation speed, which is typically small compared with the shock speed. When simulating shock-induced ignition on a regular spatial grid, the extent of reactive mixture between the leading shock and the contact surface separating fresh and inert/burnt mixture is initially zero. As the shock moves into fresh mixture, the number of grid points in the region of interest grows from one to a few. This initially poor resolution may lead to staircasing and amplification by the chemistry of initial numerical artifacts.

A novel approach which effectively overcomes that issue was proposed by Short & Dold [1], in which the original problem formulation using space x and time t as the independent variables is converted into a problem in $\eta = x/t$ and t. The initial domain becomes finite as a result and the solution is then well resolved especially at early times. Here, in addition to solving the transformed problem using a second

order ENO algorithm, the chemistry is modeled by a three-step chain-branching scheme which mimics chain-branching in hydrogen combustion. This approach appropriately handles not only the hot spot formation but its rapid growth, the birth of a secondary shock and the appearance of a detonation wave.

Below, the transformed problem and the chemical scheme is presented, then the numerical solution is briefly explained. Results for three-step chain-branching kinetics are shown, and the ignition evolution for hydrogen mixtures of different concentrations is studied in detail.

2. CONSERVATION LAWS

The problem is governed by the reactive Euler's equations. Chemistry is modeled using a three-step chain-branching scheme originally proposed by Short & Quirk [2], and used, among others by Sharpe & Maflahi [3] in previous shock-initiation studies. The three reaction steps are initiation, branching and termination. During the initiation step, the fuel, λ_1, is converted slowly into chain-radicals, λ_2. Subsequently, during the branching step, λ_1 and λ_2 react to produce more chain-radicals. The reaction proceeds to completion with the termination step in which the chain-branching specie, λ_2, is converted into products, $\lambda_3 = 1 - \lambda_1 - \lambda_2$. Initiation and branching are described by an Arrhenius rate, and termination is assumed to be constant. Upon transformation of the governing equations, and using subindex I for initiation, B for branching and T for termination chemistry can be written as:

$$\frac{\partial(t\rho\lambda_1)}{\partial t} + \frac{\partial}{\partial \eta}(\rho u\lambda_1 - \eta\rho\lambda_1) = -t\rho(r_I + r_B) \tag{1}$$

$$\frac{\partial(t\rho\lambda_2)}{\partial t} + \frac{\partial}{\partial \eta}(\rho u\lambda_2 - \eta\rho\lambda_2) = t\rho(r_I + r_B - r_T) \tag{2}$$

where

$$r_I = \lambda_1 \exp\left(\frac{E_I}{T_I} - \frac{E_I}{T}\right),\ r_B = \rho\lambda_1\lambda_2 \exp\left(\frac{E_B}{T_B} - \frac{E_B}{T}\right),\ r_T = k_T\lambda_2 \tag{3}$$

ρ is the density, u is velocity, p is pressure, e is the internal energy, E is the activation energy and T is the temperature. Temperature and internal energy are related to pressure, density, mass fractions, velocity and heat release, Q, by

$$p = \rho T, \quad e = \frac{p}{(\gamma - 1)\rho} + \frac{u^2}{2} - Q(1 - \lambda_1 - \lambda_2) \tag{4}$$

Taking the conditions between the contact surface and the shock as a reference, pressure, density and temperature are scaled by their initial postshock values as determined from the inert Riemann problem, velocity by the square root of the ratio pressure/density in the shocked fluid, heat release,internal energy and activation energy by the postshock ratio of pressure/density. Finally, time has been scaled such that the dimensionless constant termination rate is unity. In the transformed problem initial conditions consist of three uniform regions: for $\eta < \eta_s$ (the initial speed of the leading shock), unburnt fluid coming from infinity into the leading shock, shocked mixture for $\eta_s < \eta < 0$ and burnt/inert fluid in the region $\eta > 0$, separated by a temperature interface (i.e. contact surface) located at $\eta = 0$. Fresh mixture is characterized by $\lambda_1 - 1 = \lambda_2 = \lambda_3 = 0$, whereas burnt/inert mixture is characterized by

$\lambda_3 - 1 = \lambda_1 = \lambda_2 = 0$. In this way, the full resolution is available in the region between shock and contact surface already from the initial time, overcoming the difficulty due to non-existence of an initial physical domain, when solving this problem on a normal spatial domain. The dimensionless state ahead of the shock is determined as a function of the shock Mach number using the Rankine-Hugoniot equations.

$$\rho_o = \frac{(\gamma + 1)}{(\gamma - 1) + 2/M_s^2} \tag{5}$$

$$p_o = \frac{2\gamma M_s^2 - (\gamma - 1)}{\gamma + 1} \tag{6}$$

$$u_o = \frac{\sqrt{\gamma} M_s (1 - \rho_o)}{\rho_o} \tag{7}$$

To conclude the physical model, boundary conditions are taken to be consistent with the initial conditions.

3. NUMERICAL SIMULATION

The transformed problem is solved numerically using a second order accurate Essentially Non-Oscillatory (ENO) algorithm. The code was first developed by Xu et al.[5], and has since been significantly modified and parallelized to handle the shock-ignition problem. It is well-validated, as it has been used successfully in various studies [4, 6, 7, 8, 9]. In order to implement the transformation properly a new CFL condition had to be derived as this transformation brings about a troublesome side effect. At early times the characteristic speeds of the transformed system approach infinity, this restricts the numerical scheme to very small time steps initially rendering the simulation very inefficient. This issue can be amended by either starting the computation at a small positive non-zero time, or more accurately, by using a perturbation model to find an analytical solution at short times which is subsequently used as initial conditions. In this paper the latter approach was used. The resulting analytical solution is not shown here, however see [4] for a detailed derivation for single step kinetics even if the final expressions are not the same. The numerical domain goes from a negative value of η slightly smaller than η_s to a positive value rather larger than the speed of sound behind the contact surface. This guarantees that the leading shock will never reach the left boundary. Likewise, the right boundary is placed at a value greater than the speed of sound behind the contact surface so that acoustic waves moving right will never reach this boundary and no reflection occurs.

4. RESULTS

Results shown below were obtained for a shock moving away from the contact surface at a Mach number of 1.5 into premixed hydrogen-air mixtures. The parameter set used throughout this paper is

$$E_I = 20,\ E_B = 8,\ T_I = 3,\ T_B = 0.9,\ \gamma = 1.4 \tag{8}$$

with varying heat release, Q, in order to mimic mixtures with different concentrations, or equivalently increase/decrease the amount of dilution in the mixture. All cases simulated correspond to post-shock states inside the chain-branching explosion region, since the temperature behind the the shock ($T_s = 1$) is higher than the chain-branching crossover temperature T_B. The resolution used was 102,400 grid

points for η going from -2.5 to 2.5, which according to [4] is adequate. Results were obtained and are shown in detail for $Q = 2, 3, 6$, and 8.

Figures 1 to 3 show the entire ignition evolution for $Q = 2$, using pressure, temperature and mass fraction profiles. Likewise, Figs. 4 to 6, 7 to 9 and 10 to 12 do so for $Q = 3, 6$ and 8 respectively.

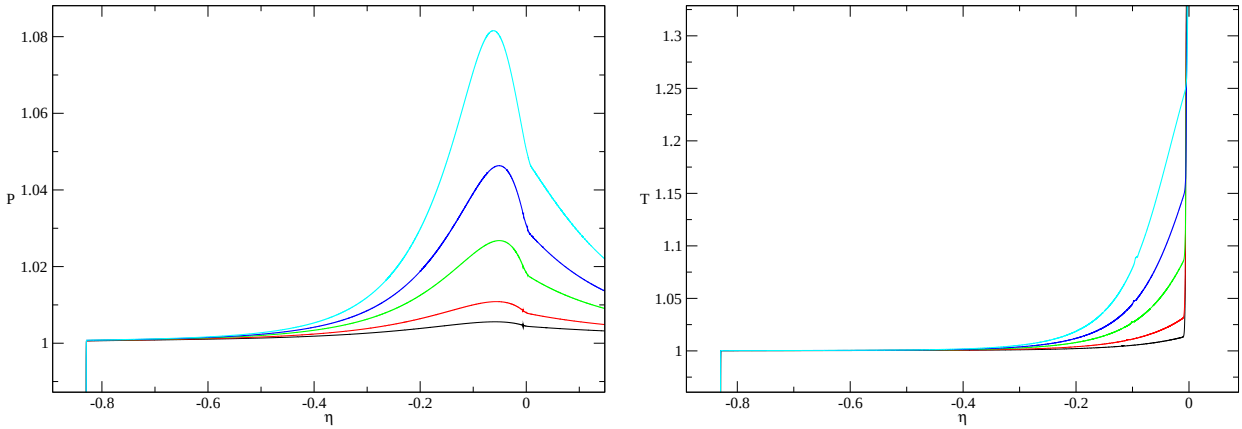

Figure 1: Hot spot formation for Q=2 at times t = 7.131, 7.727, 8.372, 8.714, and 9.071. Left: Pressure profiles. Right: Temperature profiles.

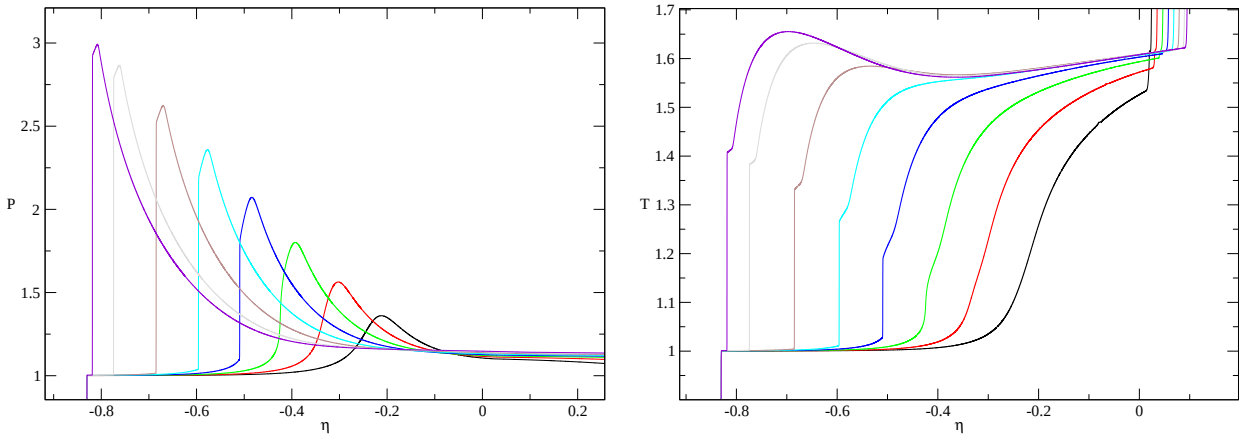

Figure 2: Transition to detonation for Q=2 at times t = 10.649, 11.538, 12.501, 13.545, 14.675, 15.901, 17.228 and 17.932. Left: Pressure profiles. Right:Temperature profiles.

Figure 1 shows the pressure and temperature profiles for the early stages of the ignition process, namely the hot spot formation for $Q = 2$. Initially, there is only a slight increase in pressure close to the contact surface, however as time goes on pressure increases more rapidly, and its maximum moves closer to it. Once ignition takes place, the maximum starts to move towards the leading shock, the pressure disturbances emanating from the reaction zone gradually amplify, steepen up, and form a secondary shock in post-shock mixture, as shown in Fig. 2. The temperatures profiles, show an interesting evolution. At the early stages of the process, the temperature maximum is always located at the contact surface, and there is little volumetric expansion induced by the chemistry as the contact surface stays essentially stationary at $\eta = 0$. With higher temperatures in this region however, the chemistry becomes stronger, and as a result the gas expands in the vicinity of the contact surface pushing it backwards. In our current frame of reference, which is attached to the contact surface, this relative movement indicates that this interface is decelerating. The maximum in pressure and temperature attained during the hot spot formation were

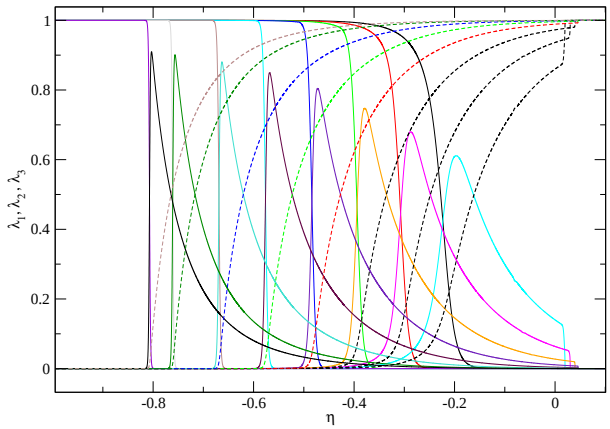

Figure 3: Mass fraction profiles for Q=2 at times t = 10.649, 11.538, 12.501, 13.545, 14.675, 15.901, 17.228 and 17.932.

1.085, and 1.25 respectively, whereas for the late stage of the process these maximums became 3 for pressure and 1.65 for temperature. For this case, there is not complete transition to detonation prior to the merging with the leading shock, as the reaction wave shown in Fig. 3 does not have time to couple with the secondary shock in this time frame. Nonetheless, a detonation will eventually develop fully and will propagate in fresh pre-shock mixture after merger (not shown). Figure 3 shows in detail the evolution of the mass fractions, the solid lines represent mass fraction of fuel, λ_1, and chain-branching specie,λ_2, whereas the dashed lines represent the mass fraction of products, λ_3. Initially, the mass fraction of fuel remains unchanged until, closer to the contact surface where intense chemistry takes place, it starts to get consumed. Subsequently, chain-branching radicals are produced as a result of fuel consumption, they reach a peak and are later depleted by the termination step. For the first profiles shown, there is significant overlap between each of the stages of the chemistry, however as time progresses, and the temperature increases the evolution becomes more chain-branching in nature, as this reaction rate dominates. This explains the increase in the peak of chain-branching specie as one moves closer to the leading shock.

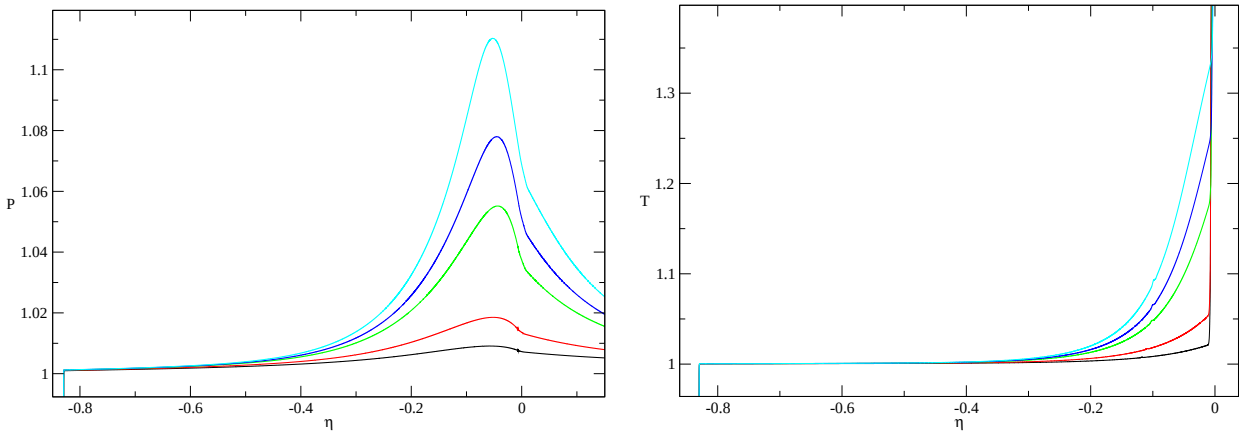

Figure 4: Hot spot formation for Q=3 at times t = 7.131, 7.727, 8.372, 8.541, and 8.714. Left: Pressure profiles. Right: Temperature profiles.

The evolution for $Q = 3$ is very similar to that explained above, with the exception of higher pressures, and temperatures, stronger chemistry and more volumetric expansion in the gas. As a matter of fact, this trend holds for the remaining values of Q simulated, as can be observed in Figs. 4 to 12. The time

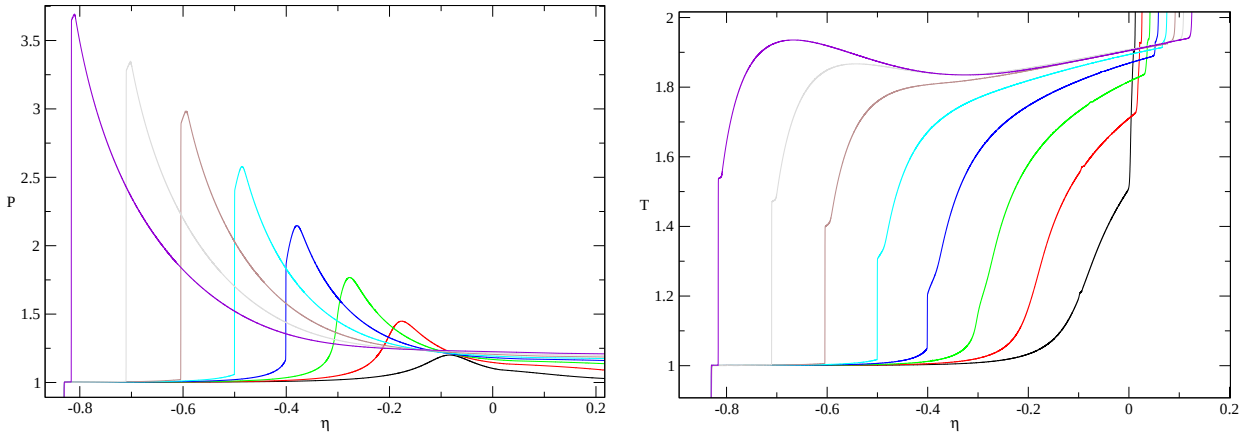

Figure 5: Transition to detonation for Q=3 at times t = 9.071, 9.828, 10.649, 11.538, 12.501, 13.545, 14.675 and 15.901. Left: Pressure profiles. Right:Temperature profiles.

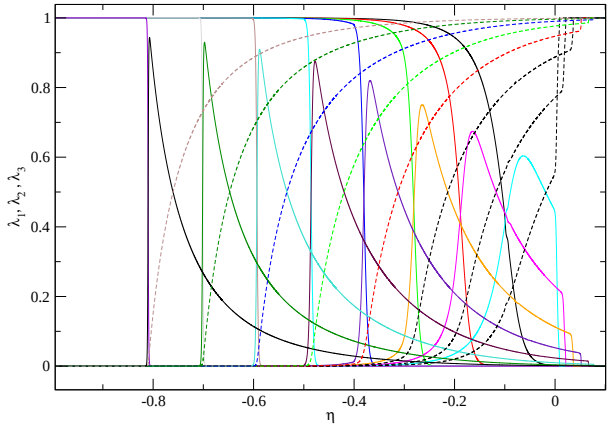

Figure 6: Mass fraction profiles for Q=3 at times t = 9.071, 9.828, 10.649, 11.538, 12.501, 13.545, 14.675 and 15.901.

for ignition to take place decreases as the mixture is less diluted, specifically it decreases from 9.071 for $Q = 2$ to 7.727 for $Q = 8$, intermediate values can be found in Figs. 4 and 7. Also the time and location where the secondary shock is born, decreases as the heat release of the mixture increases. Namely, for $Q = 2$ it forms at $\eta = -0.5$ and $t = 13.545$, for $Q = 3$ at $\eta = -0.4$ and $t = 11.538$, for $Q = 6$ at $\eta = -0.28$ and $t = 9.442$, and finally for $Q = 8$ at $\eta = -0.21$ and $t = 8.714$.

In contrast with $Q = 2$ and 3, where there was not enough time for transition to detonation to take place prior to the merging with the leading shock, for the remaining values of heat release simulated this transition did take place. The location and time where the detonation appeared were $\eta = -0.51$ and $t = 11.084$, and $\eta = -0.49$ and $t = 10.23$, for $Q = 6$ and 8 respectively.

Finally, for $Q = 3$, the maximum in pressure and temperature attained during the hot spot formation were 1.11, and 1.4 . For the late stage of the process these maximums became 3.52 for pressure and 1.91 for temperature. For $Q = 6$ were 1.16 and 1.5, during hot spot formation, and 5.3 and 2.6 for later times. Lastly, for $Q = 8$ the maximums were, during hot spot formation, 1.175 and 1.55, whereas for detonation transition were 6.3 and 3.2.

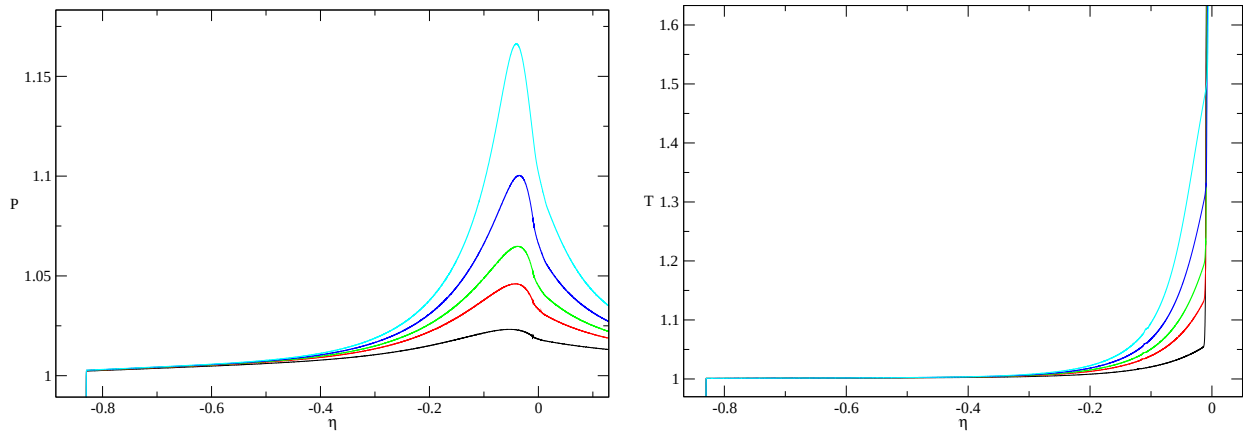

Figure 7: Hot spot formation for Q=6 at times t = 7.131, 7.573, 7.727, 7.883, and 8.042. Left: Pressure profiles. Right: Temperature profiles.

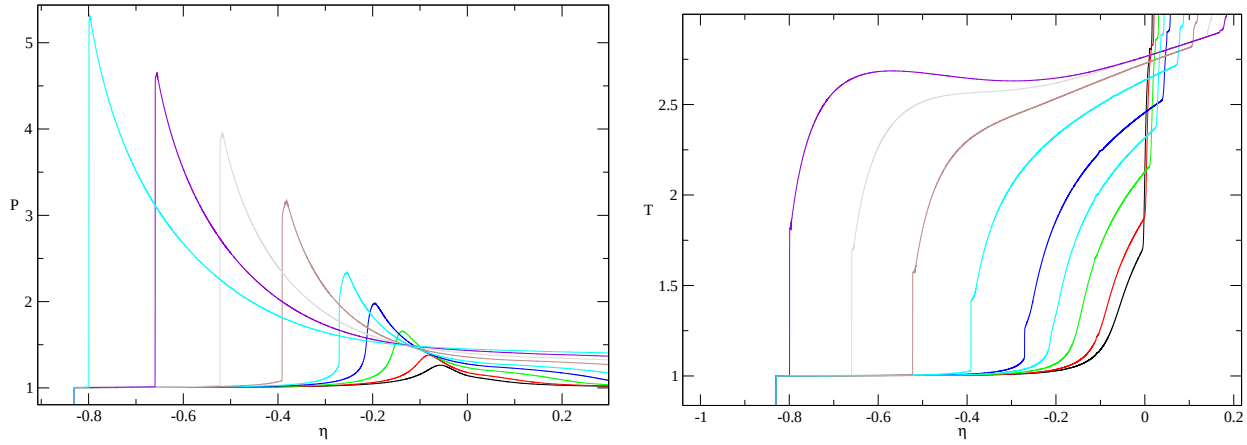

Figure 8: Transition to detonation for Q=6 at times t = 8.206, 8.372, 8.714, 9.071, 9.442, 10.230, 11.084, 12.009 and 13.012. Left: Pressure profiles. Right:Temperature profiles.

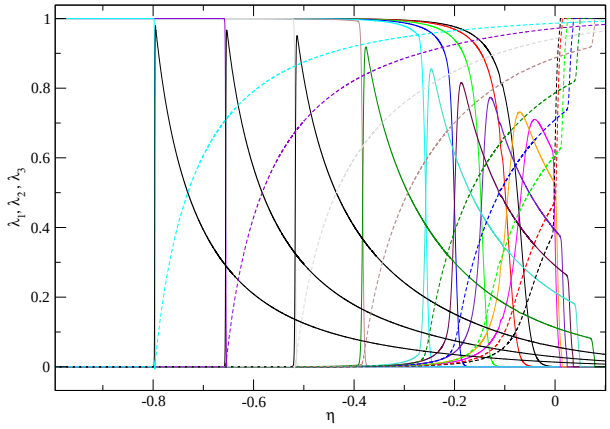

Figure 9: Mass fraction profiles for Q=6 at times t = 8.206, 8.372, 8.714, 9.071, 9.442, 10.230, 11.084, 12.009 and 13.012.

5. CONCLUSION

The scenario of shock-induced ignition was studied numerically using a three-step chain-branching kinetic scheme which attempts to model properly premixed hydrogen-air mixtures. In order to study

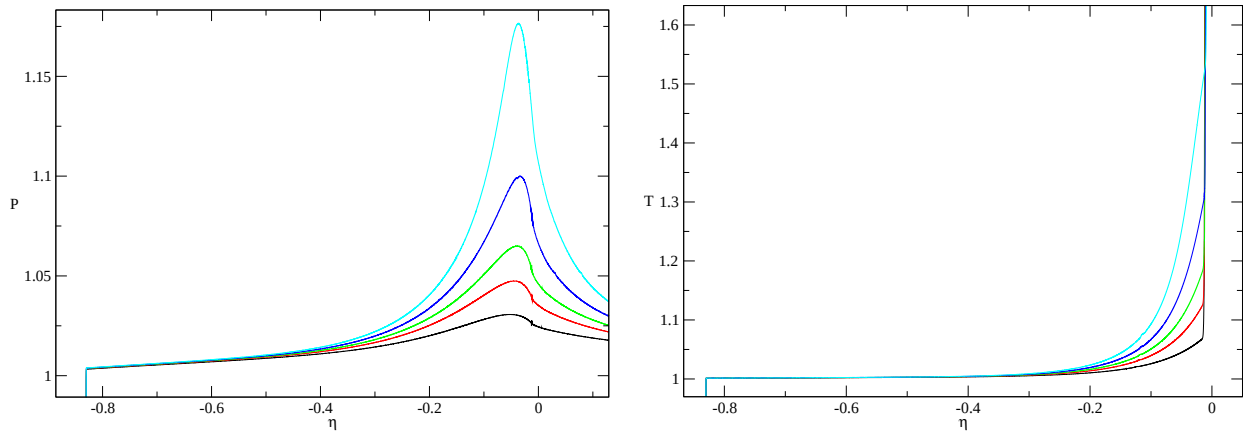

Figure 10: Hot spot formation for Q=8 at times t = 6.989, 7.276, 7.423, 7.573, and 7.727. Left: Pressure profiles. Right: Temperature profiles.

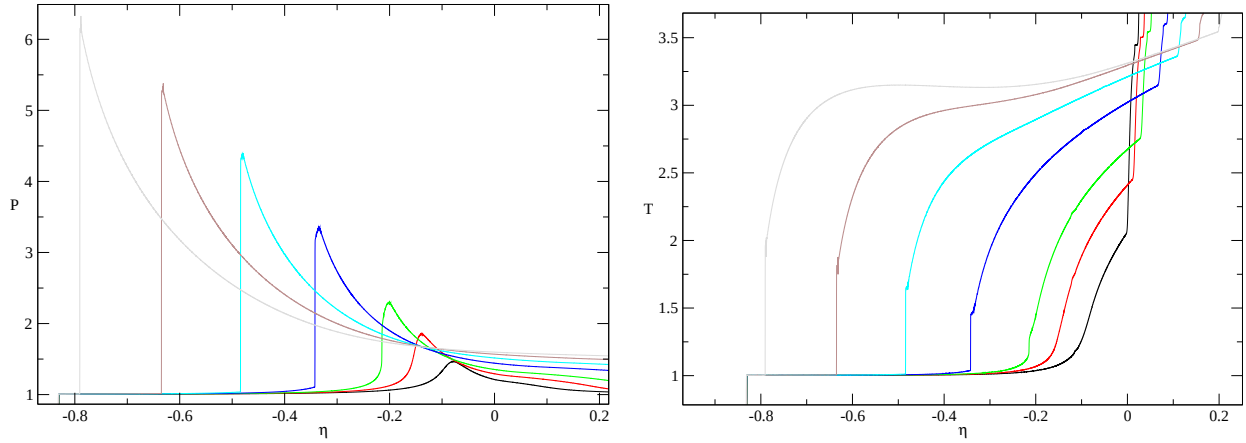

Figure 11: Transition to detonation for Q=8 at times t = 8.043, 8.372, 8.714, 9.442, 10.230, 11.084, and 12.009. Left: Pressure profiles. Right:Temperature profiles.

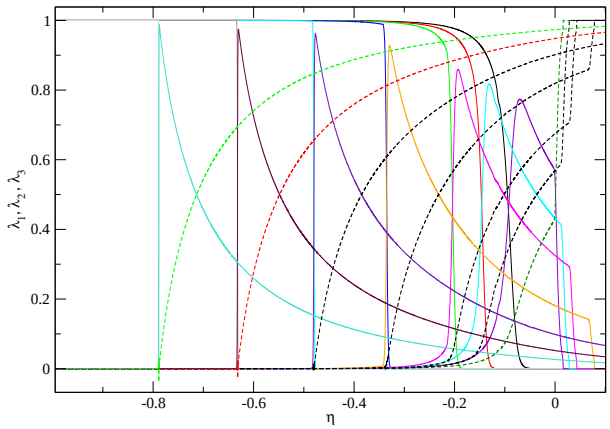

Figure 12: Mass fraction profiles for Q=8 at times t = 8.043, 8.372, 8.714, 9.442, 10.230, 11.084, and 12.009.

the effect of mixtures of different concentrations, the heat release was varied from low values, namely $Q = 2$ (i.e. highly diluted mixture) to high values, $Q = 8$. The problem was solved in a transformed

formulation, $\eta = x/t$ and t, to appropriately handle the singular nature of the initial conditions. The entire ignition evolution for all cases was explained based on pressure, temperature, and mass fractions profiles. Results show that as the heat release is increased ignition takes place faster, in addition, the location where the secondary shock forms, and a fully developed detonation appears occurs closer to the contact surface. The pressure and temperature maxima for both stages of the process, hot spot formation, and transition to detonation, attained higher values as the heat release Q was increased. For all cases simulated, except for $Q = 2$ and 3, transition to detonation took place before merging of the resulting structure with the leading shock. Finally, the approach taken proved to be effective to accurately solve the difficult problem of shock-ignition.

ACKNOWLEDGMENTS

Research supported by the NSERC Hydrogen Canada (H2CAN) Strategic Research Network, and by the NSERC Discovery Grants program.

REFERENCES

1. Short, M., Dold, W. (1996) Unsteady gasdynamic evolution of an induction domain between a contact surface and a shock wave. I: Thermal Runaway, SIAM J. Appl. Math., 56: 1295-1316.
2. Short, M., Quirk, J.J. (1997) On the non-linear stability and detonability limit of a detonation wave for a model three-step chain-branching reaction, J. Fluid Mech., 339:89-119.
3. Sharpe, G.J., Maflahi, N. (2006) Homogeneous explosion and shock initiation for a three-step chain-branching reaction model, J.Fluid Mech., 566:163-194.
4. Melguizo-Gavilanes, J., Rezaeyan, N., Lopez-Aoyagi, M. and Bauwens, L. (2010) Simulation of shock-initiated ignition. Shock Waves, doi:10.1007/s00193-010-0255-1.
5. Xu, S.J., Aslam, T., Stewart, D.S. (1997) High resolution numerical simulation of ideal and non-ideal compressible reacting flows with embedded internal boundaries. Combust. Theor. Model., 1:113-142.
6. Liang, Z. and Bauwens, L. (2005) Cell structure and stability of detonations with a pressure dependent chain-branching reaction rate model Combust. Theor. Model., 9: 193-112.
7. Bédard-Tremblay, L., Melguizo-Gavilanes, J. and Bauwens, L. (2009) Detonation structure under chain-branching kinetics with small initiation rate, Proc. Combust. Inst., 32: 2339-2347.
8. Bédard-Tremblay, L., Fang, L., Melguizo-Gavilanes, J., Bauwens, L., Finstad, P.H.E., Cheng, Z. and Tchouvelev, A.V. (2009) Simulation of detonation after an accidental hydrogen release in enclosed environments, Int. J. Hydrogen Energ., 34: 5894-5901.
9. Bauwens, L., Bauwens, C.R.L. and Wierzba, I. (2009) Oscillating flames: multiple scale analysis, Proc. R. Soc. Lond. A, 465: 2089-2110.